

Inverse stimulation enables ultrasonic binary coding for NDE using a custom linear testing system

Marius W. Schäfer^{1,*}, Sarah C.L. Fischer²

Fraunhofer IZFP, Campus E3.1, Saarbruecken, 66123, Saarland, Germany

ARTICLE INFO

Keywords:

Ultrasound
Inverse stimulation
Coded excitation
Linear system model
Binary coding

ABSTRACT

Ultrasonic testing is an established method of non-destructive evaluation. The increasing complexity of material systems requires an extension of conventional methods. In related fields such as radar and medical ultrasound, signal optimisation and coded stimulation are successfully used and offer great potential for optimising state-of-the-art measurements and extending applications. In our work, we highlight the difference between using a coded sequence to stimulate an ultrasonic testing system and the actual performance of the digital code to motivate the exploration of inverse stimulation. In order to study inverse stimulation, a custom-built ultrasonic system was designed. As a first step, the transfer function was obtained by testing pulse and chirp stimulation. In the next step, inverse stimulation was performed based on the linear transfer function to engineer the ultrasonic echoes to have shapes similar to the target code. Finally, the auto-correlation function of the ultrasonic echoes resulting from the inverse stimulation is compared with the function of the original code sequence and the agreement of the recorded ultrasonic echo with the spectrally limited code sequence. With this work we propose an integrated, low-voltage, fully linear ultrasonic testing system where the recording of a linear transfer function allows echo engineering even for a binary coded excitation sequence. We have demonstrated that inverse stimulation enables the generation of binary ultrasonic echoes with performance equal to the digital code.

1. Introduction

Ultrasonic testing is an established method with a range of applications from medical diagnostics to industrial quality control [1,2]. In the field of non-destructive evaluation (NDE), many ultrasonic techniques are based on time-of-flight measurements in contact mode. An ultrasonic transducer is coupled to a test object, a stimulation sequence is excited, and one or more backwall echoes are measured. Depending on the application, the time-of-flight provides information on material properties, material thickness, defects or stress states in the material. As inspection systems and specimens become more complex, ultrasonic techniques must be adapted.

One of the main limiting factors in ultrasonic testing is the limited capabilities of ultrasonic testing systems in terms of signal engineering. With more flexible testing systems, the excitation sequence can be changed to much more complex sequences, so-called coded excitation sequences, in order to maximise the echo information, the signal-to-noise ratio and thus to minimise the ambiguity [3–7]. However, while sequences can be selected based on their auto-correlation functions, it

has been found that this approach has limitations and requires a high level of understanding of the interplay between ultrasound, test system and test object [8].

In many cases, even expert knowledge is not sufficient and efficient to perform signal engineering and optimisation. In many cases, sequences are selected based on maximising the auto-correlation function of the excitation signal. However, this does not take into account the deformation of the resulting echoes due to ultrasonic mechanics and thus the discrepancy between the optimisation of the signals and the echoes.

We have previously shown that direct stimulation using a digital code performs well when compared to standard sinusoidal stimulation [8]. However, there is potential in exploring techniques to further improve echo engineering to the point where the auto-correlation function (ACF) of the echoes themselves is close to the ACF of the sequences. This can be achieved by so-called inverse stimulation, where the influence of the system is deconvolved from the stimulation sequence prior to excitation, so that the expected echoes actually represent the encoded sequence. The problem with direct stimulation is that

* Corresponding author.

E-mail addresses: marius.schaefer@izfp.fraunhofer.de (M.W. Schäfer), sarah.fischer@izfp.fraunhofer.de (S.C.L. Fischer).

¹ ORCID: [0000-0001-6764-7990](https://orcid.org/0000-0001-6764-7990).

² ORCID: [0000-0003-1569-276X](https://orcid.org/0000-0003-1569-276X).

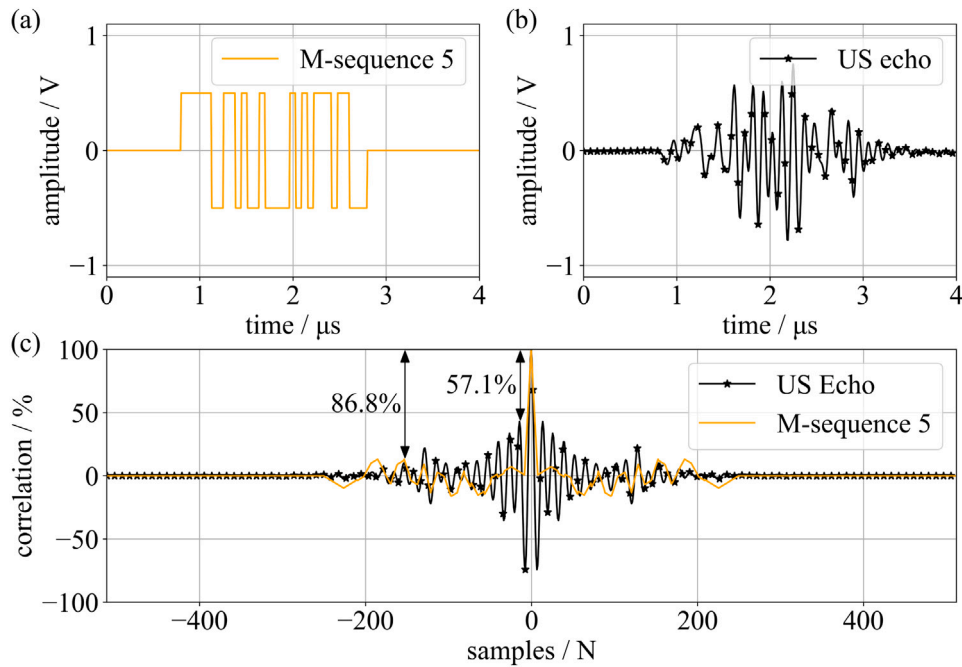


Fig. 1. Exemplary comparison of the auto-correlation function of the coded sequence and the resulting ultrasonic echo. (a) coded sequence M5, (b) recorded ultrasonic echo and (c) correlation functions of the stimulation sequence and the resulting echo.

stimulating an ultrasonic test system with a coded sequence that has a good correlation function in itself does not necessarily result in an ultrasonic echo with the same qualities. To highlight the quality of direct coded stimulation, we generate a M-sequence (or pseudo-random binary sequence) of order 5 with a resulting length of 2 μs [9,10]. The ultrasonic echoes differ from the original code as shown in Fig. 1 and therefore the correlation function is also very different. Direct stimulation using the digital code gives a good side-lobe distance for the ACF, but it is very different from the ACF of the code, which results in a higher side-lobe distance and fewer oscillations.

Inverse stimulation relies on the engineering of ultrasonic echoes through knowledge of the system transfer function (TF). There are two limiting factors to the use of inverse stimulation in today's state-of-the-art ultrasonic testing systems. Firstly, many systems use tri-state or switching output stages which introduce non-linear behaviour to the system transfer function. The second and more limiting aspect is the lack of quantisation. Inverse stimulation requires a large bandwidth with many different amplitude levels, which is impossible with tri-state technology.

Our work highlights the difference between using a coded sequence to stimulate an ultrasonic testing system and the actual performance of the digital code. Inverse stimulation, based on a system-specific transfer function, allows the generation of binary ultrasonic echoes that are equivalent in performance to the digital code. To generate the desired ultrasonic echoes, a test system capable of inverse stimulation is designed and its transfer function is determined over a wide frequency range. By spectrally dividing the band-limited transfer function from the digital code sequence, we calculate the inverse stimulation waveform to produce binary coded ultrasonic echoes. With this paper we propose an integrated, low-voltage, fully linear ultrasonic testing system where the recording of a linear transfer function allows echo engineering even for a binary coded excitation sequence.

2. Materials and methods

2.1. Ultrasonic testing system design

The ultrasonic testing system consists of custom designed electronics, an ultrasonic transducer and a test object (see Fig. 2). The

main difference to other ultrasonic systems is the completely linear behaviour achieved by building the output stage using operational amplifiers to drive the transducer in differential mode. Other technologies, such as tri-state, use electrical components as switches, adding non-linear behaviour that degrades the linear descriptibility of the entire inspection system. For our implementation, the operator can connect to the test system via Ethernet using a desktop application. As the basis for the digital part of the electronics, a Xilinx ZYNQ7000 SoC is used as part of a development board that already contains a two-channel analogue-to-digital converter (ADC) and a digital-to-analogue converter (DAC). For the digital part, we build a firmware containing an arbitrary signal generator based on a 2048 element look-up table (LUT) and a data acquisition part for recording the ultrasonic echoes.

Fully functional ultrasonic electronics also require an output stage to stimulate the transducer and receiver electronics to amplify the ultrasonic echoes. The transducer is connected in a fully differential manner to the output stage and to the receiver amplifier. For this setup a PCB (Printed Circuit Board) is designed as an add-on board to the digital system. For more information on the electrical setup, see Sections 2.1.1 and 2.1.2. More information about the piezoelectric transducer and the configuration for the experiment can be found in Section 2.2.

The system power supply is 5 V unipolar, including a ± 5 V DC/DC converter to power most of the operational amplifiers.

2.1.1. Output stage

The main requirement for the output stage is that it should be linear. In terms of quantisation and sampling of the digital signals, the DAC provides 14 bit resolution and the system operates at a frequency of 125 MHz. Many ultrasonic testing systems are equipped with MOSFET output stages. Such output stages allow the use of very high burst voltages, but the biggest problem for us is that they cannot be calculated with a linear model and only provide a quantisation of two, for bipolar operation.

As a linear output stage capable of driving a piezoelectric transducer, a transformer or an operational amplifier can be used. We will continue to use an operational amplifier output stage because a transformer based output stage also usually requires a high power input.

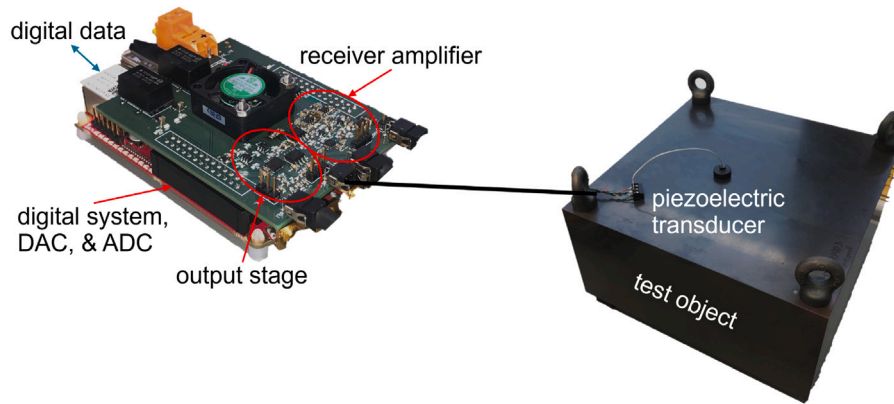


Fig. 2. Ultrasonic testing system, including build electronics, the piezoelectric transducer, and test object.

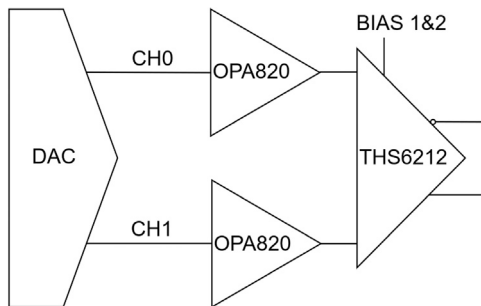


Fig. 3. Output stage circuit diagram. The BIAS pins of the driver amplifier (THS6212) are used to switch between drive mode and high impedance mode.

The schematic of the output stage is shown in Fig. 3. The two channels of the DAC output the stimulation waveform non-inverted on CH0 and inverted on CH1. The first stage of amplifiers (OPA820, Texas Instruments) is used with a gain of 2 to raise the voltage from ± 1 V after the DAC to ± 2 V, the maximum input voltage for the following component. The core component of the output stage is originally designed as a broadband differential power line communication line driver amplifier (THS6212, Texas Instruments). This device is suitable for the present application because it supports high power output for a varying electrical load and supports frequencies up to 30 MHz with low variation in overall gain. An additional feature required for this setup is the ability to disable the amplifier. The two BIAS pins can be used to switch between full driver mode and high impedance mode. It is intended that in this system an ultrasonic test can be performed using only one ultrasonic transducer. This is achieved by connecting the output stage and receiver electronics to the transducer in parallel and switching the output stage to high impedance mode when receiving. In addition, the power consumption of the system is reduced by switching off the output stage when not in use. In total, this output stage can output arbitrary signals up to ± 10 V for a load as small as 25Ω .

The inverting and non-inverting outputs are connected directly to the two sides of the piezoelectric transducer. The piezoelectric plate is isolated from the ground potential, only the shield of the cable is connected to the ground potential. An additional series resistor could be added to reduce the swing potential and to provide short-circuit protection, but this reduces the efficiency of the output stage and the other options are not necessary for this setup [11]. Also, electrical matching to the ultrasonic transducer is not as good, as we only want a constant voltage over the whole frequency range and the output stage is already capable of stimulating the transducer.

2.1.2. Receiver electronics

Like the output stage, the receiver electronics (RE) are differentially connected to the ultrasonic transducer. When a single transducer is used for evaluation, the RE is also subjected to the excitation voltage. In normal operation the RE is configured to amplify the much smaller ultrasonic echoes and the stimulation voltage would overdrive the amplifiers. A schematic of the receiver electronics circuit is shown in Fig. 4. For the first stage of amplifiers (MAX4223, Analog Devices), in addition to amplification, the device is chosen to provide an enable option. The SHDN signal is used to enable and disable the amplification of the input signals. As we are working with low voltage stimulation, this is sufficient to protect the RE input, if the RE were exposed to high voltage, an additional protection circuit is required [12].

As mentioned, the transducer operates in differential mode, so this stage is set up twice in parallel. The next stage is a differential to single-ended converter (AD8130, Analog Devices). After this conversion the path to the ADC is completed using a variable gain amplifier (AD8337, Analog Devices) and an additional amplifier ((OPA820, Texas Instruments)) to drive the ADC. A series resistor (SR) is added to reduce the potential swing between the ADC and the OPA820.

2.2. Configuration for experiments

For the following tests, the amplitude for the LUT is reduced to 0.5 V, resulting in a total stimulation voltage of ± 5 V. With this configuration, the additional DC/DC converter for the output stage could be removed and the system is only 5 V. The device under test is a $250 \text{ mm} \times 250 \text{ mm} \times 120 \text{ mm}$ block machined from 1.0045/S355JR steel and heat treated at 850°C in an inert gas atmosphere.

The ultrasonic transducer is made of a 3:1 piezoelectric composite of PZ29 (ferroperioptesoceramics) and araldite (araldite, Aradur HY 956) with a damping layer of AL₂O₃ (10 μm –100 μm particles) and araldite mixed in a 4:1 ratio. The thickness of the plate is 0.29 mm and the individual piezo rods are 0.045 mm \times 0.045 mm with a pitch of 0.08 mm. The nominal center frequency of the piezoelectric plate is 5 MHz. A 1 mil polyimide foil is attached for electrical isolation. To achieve a constant coupling to the test object, a ring magnet is used to mount the transducer, using engine oil as the coupling fluid.

The measurements were made in pulse-echo mode using a piezoelectric transducer. In pulse echo mode, the single transducer emits an acoustic wave that propagates through the test object. The wave is reflected at the back wall of the object and travels reverse to the transducer [8,13]. The transducer is switched to receiver mode and the ultrasonic echo is amplified and digitised. This is followed by data processing and spectral analysis of the ultrasonic echoes in relation to the stimulation sequences.

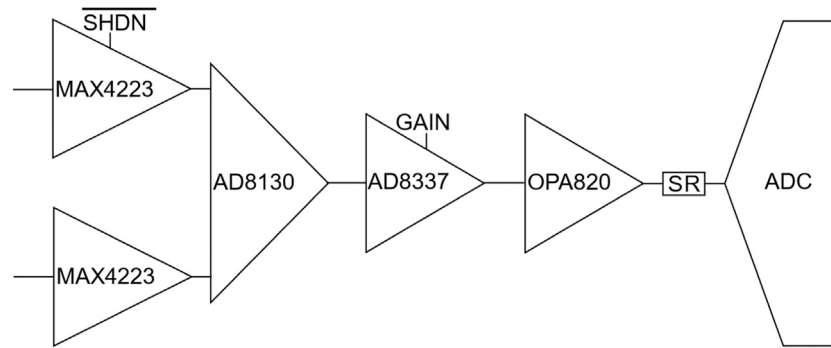


Fig. 4. Schematic of the receiver circuit.

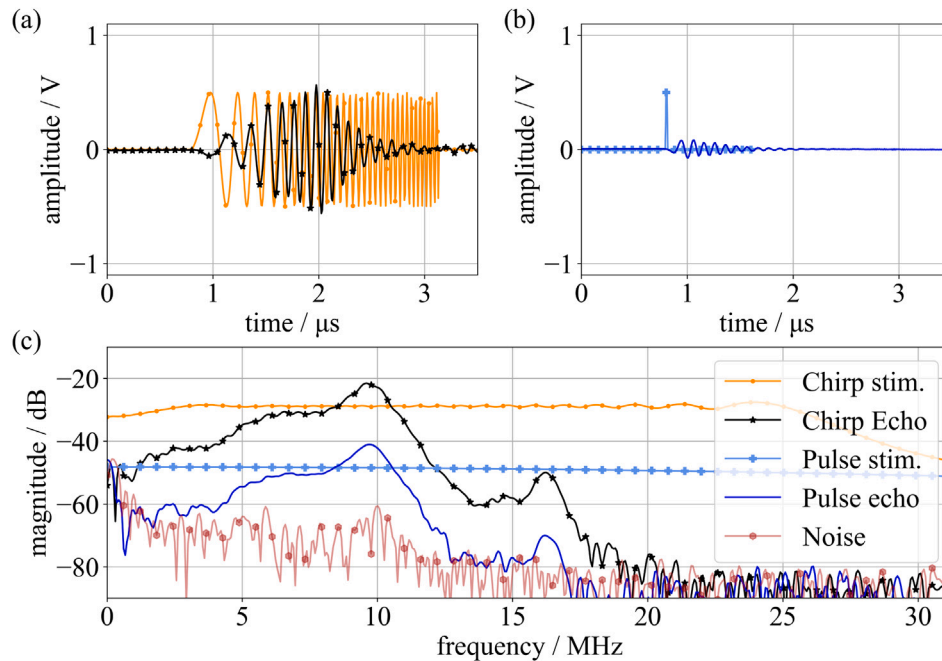


Fig. 5. Comparison of wideband chirp and pulse stimulation and response of the ultrasonic testing system. (a) Time signals for chirp stimulation and the corresponding echo. (b) Time signals for pulse stimulation and the corresponding echo. (c) Spectral magnitude representation of the stimulation sequences, ultrasonic echoes and system noise. The bandwidth for calculating the transfer function is limited where the echo magnitude falls to the noise magnitude.

3. Results and discussion

In order to study inverse stimulation using coded excitation, a custom-built ultrasonic system was designed. As a first step, the transfer function was acquired to test pulse and chirp stimulation as a basis for inverse stimulation. In the next step, inverse stimulation was performed based on the linear transfer function to design the ultrasonic echoes to have shapes similar to the target code. Finally, direct and inverse stimulation are compared in terms of their auto-correlation function and the agreement of the recorded ultrasonic echo with the spectrally limited code sequence.

3.1. Acquisition of the linear transfer function

There are many ways of obtaining a transfer function for a system [14]. In communications engineering, an impulse response is typically used to calculate the system transfer function. The impulse is used because it contains every frequency and therefore the resulting echo contains system information for the whole frequency range.

However, it is difficult to generate a pulse in an ultrasonic testing system because the output stage is always limited in its transfer capability. Instead, a high frequency pulse can be used to calculate the transfer

function for the frequency range below the pulse frequency. A second problem with using a single small pulse is the low energy input to the system. Alternatively, for a band-limited acquisition of the system transfer function, a chirp signal covering the bandwidth of interest can be used. This stimulation contains much more energy and the response is expected to provide a better signal to noise ratio (SNR).

For this study, a high frequency pulse and a broadband chirp stimulation were chosen. While pulse stimulation is the simplest method, we chose chirp stimulation as the second method because of the higher energy input.

Fig. 5 shows the stimulation sequences and the resulting echoes in the time and frequency domain. For the frequency plot, the noise recorded with the echoes is additionally plotted to highlight the SNR distance and valid ranges for the calculation of a system transfer function.

The shape of the curves for the spectral representation of the echoes is comparable for both stimulation options. The low energy input of the high frequency pulse combined with the low voltage testing system results in a poor SNR. The echo recorded from the chirp stimulation has an overall higher amplitude and therefore offers a higher frequency range before reaching the noise amplitude.

The transfer function is calculated by dividing the resulting echo by the stimulation sequence in the frequency domain. The resulting

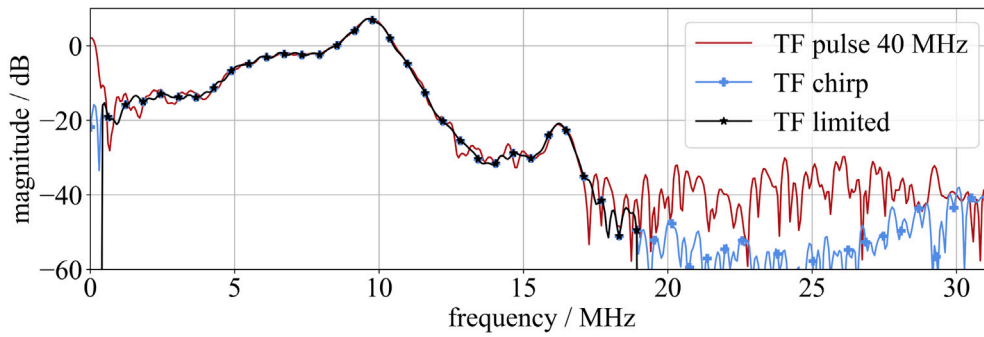


Fig. 6. System transfer function calculated from pulse and chirp stimulation and the limited TF generated from chirp stimulation using the noise limits.

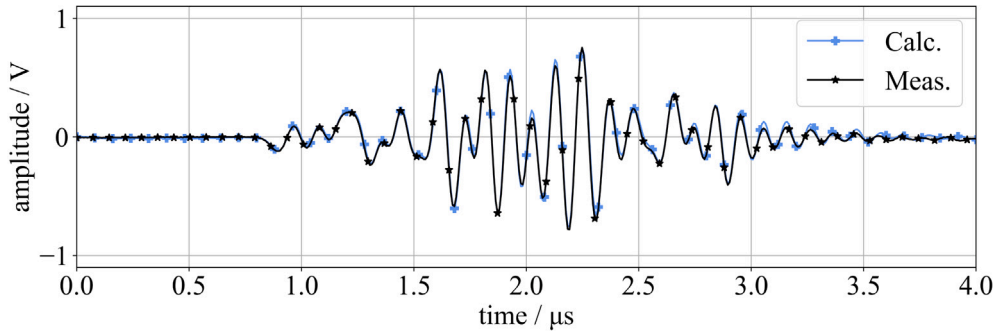


Fig. 7. Calculation and recording of the ultrasonic echo for M-sequence 5 stimulation.

curves are shown in Fig. 6. The curve produced by the chirp stimulation shows less interference from noise influence. For pulse stimulation, the resulting curve shows more noise, especially at low frequencies up to 3 MHz and high frequencies between 13 and 15 MHz. Above 16.5 MHz the noise dominates the signal. For chirp stimulation, a valid system representation is possible between 0.427 MHz and 18.981 MHz.

In frequency regions where the noise dominates the signal, the transfer function leads to miscalculation. To negate the influence of these areas on the calculation, the values of the TF curve below the noise ratio are set to 10^{-10} dB, creating a limited TF. The limited TF is created from the chirp TF using the limits presented earlier in this section due to the greater bandwidth above the noise.

To test the TF for correct representation of the ultrasonic testing system, we carry out a calculation of the ultrasonic echo for the M-sequence stimulation that we have tested in Fig. 1. Fig. 7 shows the recording of the ultrasonic echo with the test system and the result of the calculation performed with the limited TF.

The results are almost identical, so the linear TF is a good representation of the system behaviour. The resulting echo is deformed compared to the original sequence as shown earlier in Fig. 1.

The linear TF allows the calculation of ultrasonic echoes for complete arbitrary waveforms (Barker codes, chirp signals, ...). As discussed earlier, selecting a stimulation waveform that provides a good correlation function does not necessarily result in an ultrasonic echo of equal performance.

Up to this point, this work focused on the calculation of ultrasonic echoes resulting from an input sequence. To enhance the stability and ambiguity of ultrasonic measurement techniques, the following section will address a strategy to select the stimulation sequence which yields optimal echo performance by implementing the inverse stimulation. To achieve this, the calculation flow is inverted, starting with the selection of the desired ultrasonic echo, for instance the M-sequence 5, from which the required, optimal stimulation sequence is derived.

3.2. Inverse stimulation of a binary sequence

The approach for inverse stimulation is based on the experiment discussed in Section 3.1, which shows that for the linear test system, ultrasonic echo calculation is possible by spectral multiplication of the TF to the stimulation sequence. For inverse stimulation we reverse this process and divide the TF from the stimulation sequence and use the resulting time signal for stimulation. Due to the large gain difference over the bandwidth of the TF, the resulting echo is expected to be quite small. To reduce this effect in a second approach, we reduce the maximum frequency of the valid TF to limit the gain difference to the low frequency gain, resulting in a maximum frequency of 13.672 MHz.

Fig. 8(c) shows the spectral representation of the M-sequence and the two resulting curves for the calculation of the inverse stimulation sequence. Fig. 8(a) and (b) show the two resulting time sequences used to stimulate the ultrasonic system in the next step. It should be noted that we have circularly shifted the resulting sequences by 1024 elements (half the length of the LUT) in order to place them in the centre of the LUT.

The resulting records of the ultrasonic echoes and the original code sequence are shown in Fig. 9. For both configurations shown in Fig. 8, the resulting signals shown in Fig. 9 agree very well with the expected code sequence. For the full bandwidth of the TF tested in 9(a) the resulting amplitude is, as expected, lower than for the more limited test shown in 9(b) and the influence of noise is therefore greater. A look at Fig. 9(c) shows almost identical correlation functions for the code and the recorded ultrasonic echoes. The side-lobe distance of the code is 86.8% and that of the ultrasonic echoes is 84.3% and 82.7% respectively.

Although the correlation function is almost identical, the ultrasonic echoes do not match the code sequence perfectly. There is a negative drift at the beginning of the echo and the amplitude limit for the start pulse is not reached.

The analog transmission of perfect rectangular changes, like the jumps in the M-sequence, would require infinite bandwidth, which is

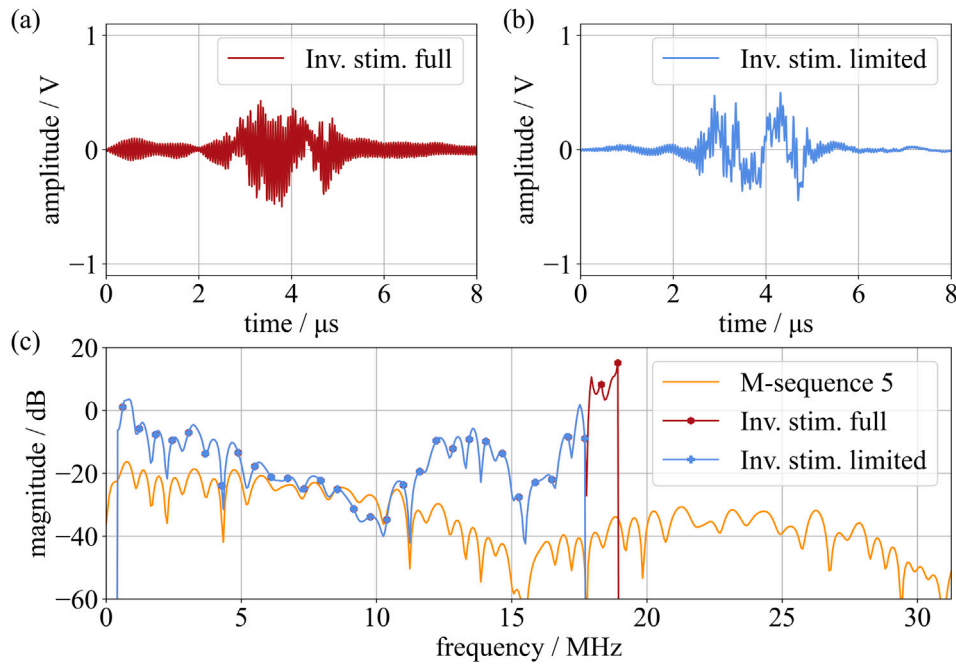


Fig. 8. The inverse stimulation sequence for the M-sequence 5. A calculated stimulation sequence is re-scaled to 0.5 V which gives the maximum amplitude for the output stage. (a) shows the result using the full bandwidth described in Section 3.1 and (b) the result using a smaller bandwidth to reduce the maximum gain difference. (c) shows the spectral magnitude representation of the M-sequence and the two stimulation sequences for inverse stimulation.

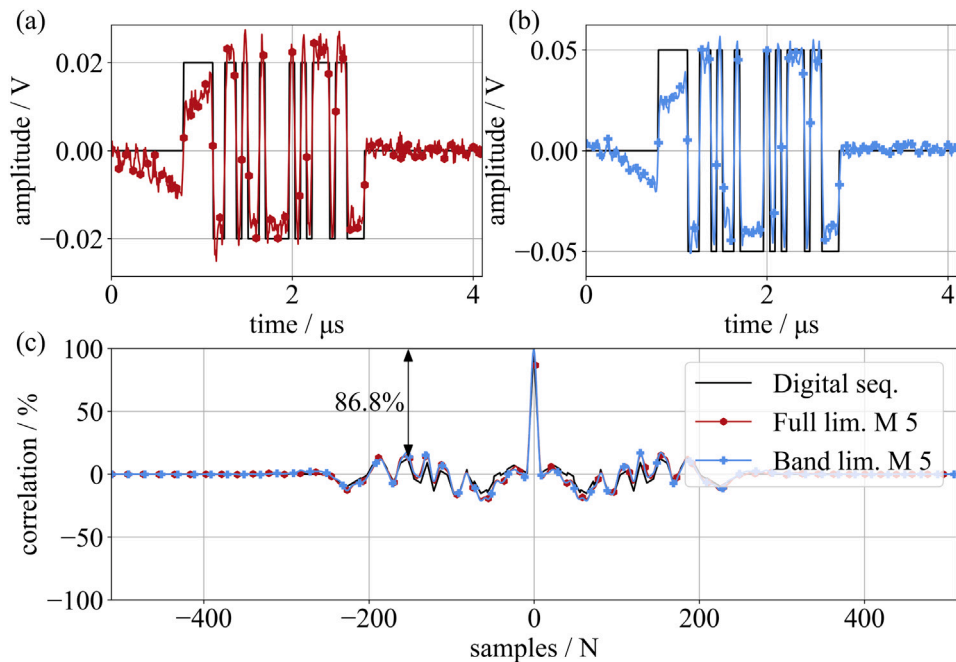


Fig. 9. (a) Ultrasonic echo using the bandwidth of Section 3.1 and M-sequence 5 . (b) M-sequence and ultrasonic echo using the smaller bandwidth, resulting in higher amplitude with less noise influence. (c) ACF of the digital sequence and the two ultrasonic echoes shown in (a) and (b).

not possible with real electrical components. In this work, the maximum frequency used for the calculation of the transfer function and the inverse stimulation sequence is determined based on the noise distance. This limits the sharpness of potential edges in the resulting ultrasonic echoes [15,16]. To support this hypothesis, the lower spectral limit is applied to the coded sequence and compared with the corresponding ultrasonic echo. Fig. 10 shows the ultrasonic echo for the smaller bandwidth case and the coded sequence using the same spectral limit.

Taking into account the noise, the two waveforms match well. The maximum normalised cross-correlation is 98.37%.

In comparison to the direct stimulation, the presented ultrasonic echoes for the inverse stimulation demonstrate an equivalent performance in terms of the correlation function to that of the original code. A portion of the discrepancy in the time signal can be attributed to the spectral limitation. Additionally, the deviation is influenced by noise in two different ways. Firstly, the system is operating at lower amplitudes

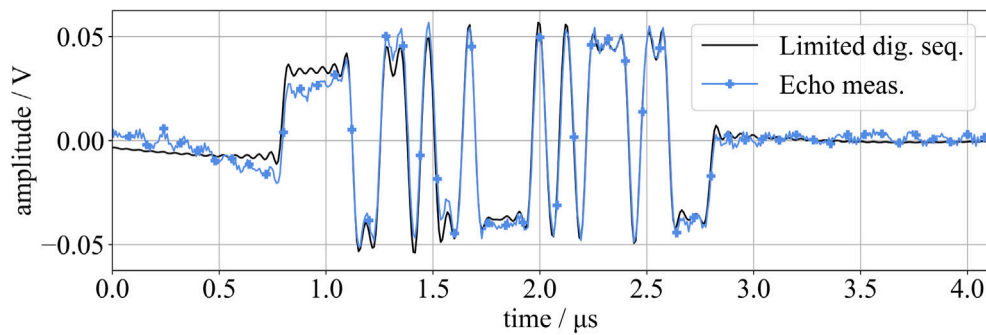


Fig. 10. Ultrasonic echo for the smaller bandwidth and the digital M-sequence with the same spectral limit.

and therefore closer to the noise level, so the direct influence of the noise is visible. Secondly, the inversion of a strictly proper TF implies a differentiation, which results in an amplification of the noise [17].

In conclusion, we have shown that inverse stimulation allows the full potential of a coded sequence to be exploited directly within the recorded ultrasonic echo.

3.3. Discussion

With this work, we have addressed many points for future improvement in ultrasonic testing based on inverse stimulation, which maximises the quality of the cross-correlation function of the echoes rather than that of the stimulation sequence. We have shown that our ultrasonic testing system can be fully described by a linear model based on a single measurement. The quality of this representation is such that it can compute the inverse stimulation of a binary sequence and generate a binary ultrasonic echo that exploits the full potential of the coded sequence.

The signal properties in terms of ambiguity or stability of digitally coded ultrasonic echoes are superior compared to currently used stimulation options. This provides a solution to current ambiguity-based problems, such as the stability of a screwdriving process described by [18]. A second application could be defect location by calculating the transfer function for the backwall echo. The exact position of defects can be located more accurately and reliably. In addition, this offers the possibility of performing a single-shot channel calibration for a single channel in an ultrasonic testing system. With inverse stimulation, the ultrasonic echo equals the desired coded sequence, reducing reconstruction to a minimum.

There are several ways in which this method can be used to increase the amount and quality of information obtained from a test object. The direct use of this method is to include the specimen in the transfer function determination and use an evaluation method that uses two ultrasonic echoes or subsequent measurements. The deviation between the first and second ultrasonic echoes is caused only by the specimen and this information is maximised because the influence of the test system, including the electronics and transducer, is compensated for in both echoes. In a slightly different way, compensation can be made using a reference specimen, either by keeping the reference specimen in the TF or by mathematically removing its influence and then switching to the actual specimen.

If the constraints are suitable for the process, a code selection must be made. The choice of code will depend on the test case and the capabilities of the testing system. The possible length of a coded sequence is limited by the excitation frequency and the time slot between the start of transmission and the reception of the ultrasonic echo. After recording the system transfer function, the spectral band limit is applied depending on the noise distance and the tolerated gain gap. The minimum factor bandwidth required to transmit a binary coded sequence can be approximated by checking the quotient of the widest and smallest pulse. The use of the linear ultrasonic testing

system makes it possible to accurately calculate the resulting ultrasonic echo for inverse stimulation, thus allowing the stimulation sequences to be specifically tailored to the test case.

In addition, we have shown that a 5 V-only inspection system can be built in a small space, reducing material costs and improving energy efficiency. When considering actual applications in multi-channel ultrasonic testing for array systems, this could mean an immense reduction in transmitter electronics and power supply.

Although there are several potential applications where inverse stimulation has the potential to improve methods, limitations must be considered. Due to the spectral gain difference, the resulting ultrasonic echoes have a low amplitude, making them susceptible to noise. In addition, the approach requires a fully linear test system and a high bandwidth, depending on the desired echo shape. For perfect representation of a binary ultrasonic echo, a higher bandwidth is required.

One strategy to avoid this problem is to reverse the process and perform the spectral division of the transfer function on the ultrasonic echo resulting from direct stimulation using the code sequence.

4. Conclusion and outlook

The most important findings of this paper are:

- determining the transfer function of a linear ultrasonic testing system from a single measurement
- highly accurate ultrasonic echo prediction, even for complex direct stimulated coded excitation sequences
- inverse stimulation of a binary ultrasonic echo results in echoes with characteristics similar to binary code sequences
- a 5 V-only testing system is built, saving space and reducing material costs, while improving energy efficiency and achieving sufficient performance using inverse stimulation

In conclusion, this approach can be utilised for regular ultrasonic testing to maximise the information about the specimen by minimising the influence of the ultrasonic testing system. For future multi-transducer ultrasonic testing in combination with binary coded ultrasonic echoes, another strategy is to introduce coded signals designed for decorrelation [19] into the process. This could permit the simultaneous use of multiple transducers with the ability to deconstruct a summed echo to the specific channels. The utilisation of inverse stimulation in conjunction with a series of orthogonal coded sequences could facilitate a further enhancement in execution speed, while concomitantly improving the sharpness and image quality [20] for matrix-based ultrasonic techniques, such as phased array or total focus [21].

Misardis looked at increasing the frame rate for medical ultrasonic imaging using quasi-orthogonal linear FM signals [22]. The use of code division multiple access for ultrasonic matrix arrays was recently exploited by Park [23,24] to reduce crosstalk for modulated coded sequences in NDT. Fan presented a convolution of Barker and Golay codes for low voltage ultrasonic testing [25] with pending hardware for

performance testing in the real test scenario and a method for nonlinear carrier modulation [26] to improve axial resolution and contrast ratio for ultrasonic imaging. For the presented modulated signals, either the signal containing the carrier is evaluated without using the full potential of the coded sequence, or additional computational effort is required to extract the coded sequence from the ultrasonic echo. Including the inverse stimulation to these applications enables the full potential of the code sequences, while keeping the computational effort at a minimum.

Building on our findings, further studies are needed to explore the advantages of inverse stimulation and coded excitation and then apply them to specific applications. A key aspect to be explored is the minimisation of ambiguity to improve the stability of a screwdriving process. In addition, the potential of coded excitation sequences for multi transducer systems needs to be demonstrated to explore how this technique can improve the execution speed and sharpness of imaging ultrasonic techniques.

CRedit authorship contribution statement

Marius W. Schäfer: Writing – original draft, Visualization, Validation, Software, Methodology, Formal analysis, Conceptualization. **Sarah C.L. Fischer:** Writing – review & editing, Supervision, Methodology, Funding acquisition, Conceptualization.

Declaration of competing interest

The authors declare the following financial interests/personal relationships which may be considered as potential competing interests: Dr. Ing. Sarah C.L. Fischer reports financial support was provided by a Fraunhofer Society for the Advancement of Applied Research. If there are other authors, they declare that they have no known competing financial interests or personal relationships that could have appeared to influence the work reported in this paper.

Data availability

Data will be made available on request.

Acknowledgments

This work was supported by the Fraunhofer Internal Programs under Grant No. Attract 025-601314.

References

- [1] F. Honarvar, F. Salehi, V. Safavi, A. Mokhtari, A.N. Sinclair, Ultrasonic monitoring of erosion/corrosion thinning rates in industrial piping systems, *Ultrasonics* 53 (7) (2013) 1251–1258, <http://dx.doi.org/10.1016/j.ultras.2013.03.007>.
- [2] S. Yang, L. Zhang, J. Fan, Measurement of axial force of bolted structures based on ultrasonic testing and metal magnetic memory testing, in: *Advances in Condition Monitoring and Structural Health Monitoring*, in: *Lecture Notes in Mechanical Engineering*, Springer Singapore and Imprint: Springer, Singapore, 2021, pp. 625–635.
- [3] R. Zetik, J. Sachs, R. Thomä, UWB short-range radar sensing - The architecture of a baseband, pseudo-noise UWB radar sensor, *IEEE Instrum. Meas. Mag.* 10 (2) (2007) 39–45, <http://dx.doi.org/10.1109/MIM.2007.364960>.
- [4] F. Herzel, A. Ergintav, G. Fischer, A novel approach to fractional-N PLLs generating ultra-fast low-noise chirps for FMCW radar, *Integration* 76 (2021) 139–147, <http://dx.doi.org/10.1016/j.vlsi.2020.09.009>.

- [5] T. Misaridis, J.A. Jensen, Use of modulated excitation signals in medical ultrasound. Part II: Design and performance for medical imaging applications, *IEEE Trans. Ultrason. Ferroelectr. Freq. Control* 52 (2) (2005) 192–207, <http://dx.doi.org/10.1109/TUFFC.2005.1406546>.
- [6] M.H. Pedersen, T.X. Misaridis, J.A. Jensen, Clinical evaluation of chirp-coded excitation in medical ultrasound, *Ultrasound Med. Biol.* 29 (6) (2003) 895–905, [http://dx.doi.org/10.1016/S0301-5629\(02\)00784-6](http://dx.doi.org/10.1016/S0301-5629(02)00784-6).
- [7] E. Vienneau, B. Byram, Compound barker-coded excitation for increased signal-to-noise ratio and penetration depth in transcranial ultrasound imaging, in: 2020 IEEE International Ultrasonics Symposium, IUS, 2020, pp. 1–4, <http://dx.doi.org/10.1109/IUS46767.2020.9251650>.
- [8] M. Schäfer, H. Theado, M.M. Becker, S.C.L. Fischer, Optimization of the unambiguity of cross-correlated ultrasonic signals through coded excitation sequences for robust time-of-flight measurements, *Signals* 2 (2) (2021) 366–377, <http://dx.doi.org/10.3390/signals2020023>.
- [9] S.W. Golomb, Shift register sequences – a retrospective account, in: G. Gong, T. Helleseth, H.-Y. Song, K. Yang (Eds.), *Sequences and their Applications – SETA 2006*, Springer Berlin Heidelberg, Berlin, Heidelberg, 2006, pp. 1–4.
- [10] R.J. McEliece, The theory of m-sequences, in: *Finite Fields for Computer Scientists and Engineers*, Springer US, Boston, MA, 1987, pp. 151–167, http://dx.doi.org/10.1007/978-1-4613-1983-2_10.
- [11] H. Göbel, *Einführung in die Halbleiter-Schaltungstechnik*, Springer Vieweg, Berlin, Heidelberg, 2019.
- [12] J. Sanchez, P. Leturcq, P. Austin, R. Berriane, M. Breil, C. Anceau, C. Ayela, Design and fabrication of new high voltage current limiting devices for serial protection applications, in: 8th International Symposium on Power Semiconductor Devices and ICs. ISPSD '96. Proceedings, 1996, pp. 201–205, <http://dx.doi.org/10.1109/ISPSD.1996.509481>.
- [13] J. Krautkrämer, H. Krautkrämer, Pulse-echo method, in: *Ultrasonic Testing of Materials*, Springer Berlin Heidelberg, Berlin, Heidelberg, 1983, pp. 193–264, http://dx.doi.org/10.1007/978-3-662-02357-0_11.
- [14] G.-B. Stan, J.-J. Embrechts, D. Archambeau, Comparison of different impulse response measurement techniques, *J. Audio Eng. Soc.* 50 (4) (2002) 249–262.
- [15] I. Trots, A. Nowicki, M. Postema, Ultrasound image improvement by code bit elongation, *IEEE Signal Process. Lett. PP* (2017) 1, <http://dx.doi.org/10.1109/LSP.2017.2776040>.
- [16] I. Trots, A. Nowicki, Influence of the transducer bandwidth on compressed ultrasonic echoes, *Arch. Acoust.* 32 (2007) 903–915.
- [17] O. Dhaou, L. Sidhom, I. Chihi, A. Abdelkrim, On the numerical differentiation problem of noisy signal, *Proc. Eng. Technol.* 2016 (2016) 423–429.
- [18] S. Herter, S. Youssef, M.M. Becker, S.C.L. Fischer, Machine learning based preprocessing to ensure validity of cross-correlated ultrasound signals for time-of-flight measurements, *J. Nondestruct. Eval.* 40 (1) (2021) 1–9, <http://dx.doi.org/10.1007/s10921-020-00745-7>.
- [19] K. Yang, Y.-K. Kim, P. Vijay Kumar, Quasi-orthogonal sequences for code-division multiple-access systems, *IEEE Trans. Inform. Theory* 46 (3) (2000) 982–993, <http://dx.doi.org/10.1109/18.841175>.
- [20] H.-W. Xie, H. Guo, G.-Q. Zhou, N.Q. Nguyen, R.W. Prager, Improved ultrasound image quality with pixel-based beamforming using a Wiener-filter and a SNR-dependent coherence factor, *Ultrasonics* 119 (2022) 106594, <https://www.sciencedirect.com/science/article/pii/S0041624X21002158>.
- [21] Sumana, A. Kumar, Phased array ultrasonic imaging using angle beam virtual source full matrix capture-total focusing method, *NDT & E Int.* 116 (2020) 102324, <http://dx.doi.org/10.1016/j.ndteint.2020.102324>, URL <https://www.sciencedirect.com/science/article/pii/S0963869520301171>.
- [22] T.X. Misaridis, J.A. Jensen, Space-time encoding for high frame rate ultrasound imaging, *Ultrasonics* 40 (1) (2002) 593–597, [http://dx.doi.org/10.1016/S0041-624X\(02\)00179-8](http://dx.doi.org/10.1016/S0041-624X(02)00179-8).
- [23] G.-R. Park, S.-H. Park, K.-R. Baek, Frequency sweep keying CDMA for reducing ultrasonic crosstalk, *Sensors* 22 (12) (2022) <http://dx.doi.org/10.3390/s2212462>.
- [24] G.-R. Park, S.-H. Park, K.-R. Baek, Improved frequency sweep keying CDMA using faster R-CNN for extended ultrasonic crosstalk reduction, *Sensors* 23 (23) (2023) <http://dx.doi.org/10.3390/s23239550>.
- [25] Z. Fan, J. Rudlin, G. Asfis, H. Meng, Convolution of Barker and Golay codes for low voltage ultrasonic testing, *Technologies* 7 (4) (2019) <http://dx.doi.org/10.3390/technologies7040072>.
- [26] Z. Fan, H.-Y. Meng, Coded excitation with nonlinear frequency modulation carrier in ultrasound imaging system, in: 2020 IEEE Far East NDT New Technology & Application Forum, FENDT, 2020, pp. 31–35, <http://dx.doi.org/10.1109/FENDT50467.2020.9337517>.